Application of Improved Numerical Techniques to the Tsunami Response of Island Systems

GERALD T. HEBENSTREIT[1]

Cooperative Institute for Research in Environmental Sciences, University of Colorado, Boulder 80309

EDDIE N. BERNARD[2]

Pacific Tsunami Warning Center, National Weather Service, Ewa Beach, HI 96706

ANDREW C. VASTANO

Department of Oceanography, Texas A&M University, College Station 77843

7 July 1978 and 15 October 1979

ABSTRACT

A finite-difference numerical model based on the classical linear long-wave equations has been developed to study the tsunami response of multiple-island systems. The first application of this model was to the Hawaiian Islands. Early results were satisfactory. However, one drawback to the model was the use, at the outer open boundaries of the basin, of a radiation condition which allowed only wave energy approaching the boundary at a normal angle to pass out of the basin without reflection. Recently, an improved boundary condition has been employed which takes into account the radial propagation of scattered waves near the boundary. The earlier model tests were repeated using this new condition. The major features of the results remained relatively unchanged. Certain secondary features of the response, which had made analysis of model results quite complicated, were either eliminated or greatly reduced.

1. Introduction

Recent studies of tsunami interaction with islands (Vastano and Bernard, 1973; Bernard and Vastano, 1977) have verified the existence of an accurate finite-difference model for studying wave resonances generated by an incident wave train with a broadband spectrum entering a multiple-island system. The first application of this model was to the Hawaiian island chain (Bernard and Vastano, 1977). The results obtained from the model indicated that these islands are susceptible to intense resonances at ten wave periods in the 12–90 min range. This band contains most of the normal tsunami periods. One drawback to the model was the use of an open outer boundary condition which fails to closely approximate the radiation of scattered wave energy (outward) from the system. Reid and Mungall (1980) recently developed an improved radiation-type boundary condition which greatly alleviates the problem. In this note we reexamine the test situation presented by Bernard and Vastano (1977) and show how the new boundary condition has improved the model results.

2. The model test

The linear equations of motion and continuity for long waves in water of varying depth are the basis for the finite-difference model. These are, in Cartesian coordinates,

$$\frac{\partial u}{\partial t} + g\frac{\partial \eta}{\partial x} = 0, \tag{1}$$

$$\frac{\partial v}{\partial t} + g\frac{\partial \eta}{\partial y} = 0, \tag{2}$$

$$\frac{\partial \eta}{\partial t} + \frac{\partial}{\partial x}(uH) + \frac{\partial}{\partial y}(vH) = 0. \tag{3}$$

The quantity H is the depth below mean water level in the basin at rest, η is the disturbance about the mean water level, and u and v are water particle velocities in the x and y directions. The linear equations are assumed to be valid throughout the basin. Bernard and Vastano discussed the finite-difference algorithm for (1)–(3) in detail.

The submarine topography surrounding the eight major islands in the Hawaiian chain was interpolated onto a 5.5 km numerical grid from depth soundings on National Ocean Survey Chart 4102. The shallowest depth allowed was 50 m, which was taken to be the depth at the island shoreline. The islands rose vertically through the surface at the 50 m contour and incident waves were totally reflected from the island shores. Thus waves could undergo multiple reflections, diffraction, refraction and partial trapping (Longuet-Higgins, 1967), but not experience energy dissipation due to run-up, bottom friction and other nonlinear processes. The strictly linear nature of the model precludes the use of model results to

[1] Present affiliation: Science Applications, Inc., McLean, VA 22102.

[2] Present affiliation: Pacific Marine Environmental Laboratories, NOAA, Seattle, WA 98105.

0022-3670/80/071134-07$05.75

predict accurate wave heights in inundation zones on the island shores; indeed, the model was not intended to produce such information.

Knowles and Reid (1970) showed that the response of an island to incident waves over a wide range of periods could be readily analyzed by using a time series input with a sufficiently broad spectrum, and with the simulation continued long enough for the wave field to come to statistical equilibrium. Bernard and Vastano used this technique to excite the Hawaiian chain and generate wave height time series at each shoreline point. They Fourier analyzed these time series and, by normalizing the resulting spectra by the spectrum of the input, they calculated response functions (output energy/input energy) at each shore point for a period range of 12.5 to 512 min. They calculated average response functions for each island, as well as an overall average for all 235 shore points. Contours of (energy ratio)$^{1/2}$ around the perimeter of each island were also produced.

3. Outer boundary condition

The outer boundary condition originally employed in the model took the form

$$\frac{\partial \eta_s}{\partial t} + \frac{c\,\partial \eta_s}{\partial n} = 0, \tag{4}$$

where η_s is the height of the scattered portion of the wavefield at the boundary (scattered height = total height − incident height), c is the wave phase speed calculated from the water depth H at the boundary, and n is a coordinate normal to and outward from the boundary. The purpose of (4) is to allow scattered wave energy to radiate outward from the rectangular model grid without reflection back toward the interior. However, this will only be accomplished if the outgoing waves approach at an angle normal to the boundary. Waves which approach at an oblique angle will undergo partial reflection, since only the outward normal component is resolved in (4). Waves which have been scattered by a reflecting barrier tend to spread radially outward and rarely will such a spreading wave front uniformly approach the outer boundary at a normal angle of incidence. Thus the original version of the Hawaiian Island model could be expected to produce results which were to some extent affected by the reflections caused by the outer boundary condition.

Reid and Mungall (1980) presented a modification to (4) which does allow radially spreading waves to scatter outward through a rectangularly bounded system. Additional studies which we conducted have shown that this new boundary condition produces satisfactory results, not only for the case of purely scattered waves, but also for cases in which the wave field consists of both forced and scattered waves. The Hawaiian Island chain cannot be considered a point scattering source; however, preliminary work with this new boundary condition indicates that it also performs well with such a broad obstacle in the path of the incident waves.

The form of the new boundary condition applied to the model is

$$v_s = \frac{g\eta_s}{c} + \frac{g}{2r}\int_0^t \eta_s dt, \tag{5}$$

where v_s is the radial component of scattered wave velocity at the boundary and r is the radial distance from an inner reference point to the boundary point. The integral term in (5) includes the influence of wave spreading.

The quantities v_s, r, and $\int_0^t \eta_s dt$, which were not needed when the outer boundary was governed by (4), required modifications to the program. The value of the integral was obtained by storing the cumulative sum of the scattered wave heights from time $t = 0$ to the time step $t - \Delta t$ for each boundary point. Values of r were calculated by referencing points on the boundary to the center of the model grid. The islands are not centered on the grid, but Reid and Mungall showed that the reference point could be a reasonable distance from the scattering source without significantly altering the results. The reference point for the Hawaiian Island model was placed at the center of the numerical grid, at a point roughly 20°N, 157°W. The complicated topography prevented analytical study of the basin, but an analysis of a flat bottom basin of identical size showed that if the true scattering center were somewhere in the area between Oahu and Maui, the reflection coefficient at the boundary due to the mismatch between scattering center and basin center would be no more than 8%.

The radial velocity component v_s required a knowledge of both the speed and direction of the scattered waves at the boundary. The direction angle was defined as that formed by the appropriate radius vector and an outward normal at the boundary point. Since, for the particular tsunami approach azimuth chosen for study, the forcing wave always propagated normal to the northern edge of the grid and parallel to the eastern and western edges, the scattered wave speed could be readily determined from the total (forced and scattered) wave velocity field along the boundaries.

4. Model results

In this section we will compare our model results with the results presented earlier. Figure references here will include (in parentheses) the number of the comparable figure in the original paper (Bernard and Vastano, 1977). In order to allow comparison between the two tests, the basin size [including the

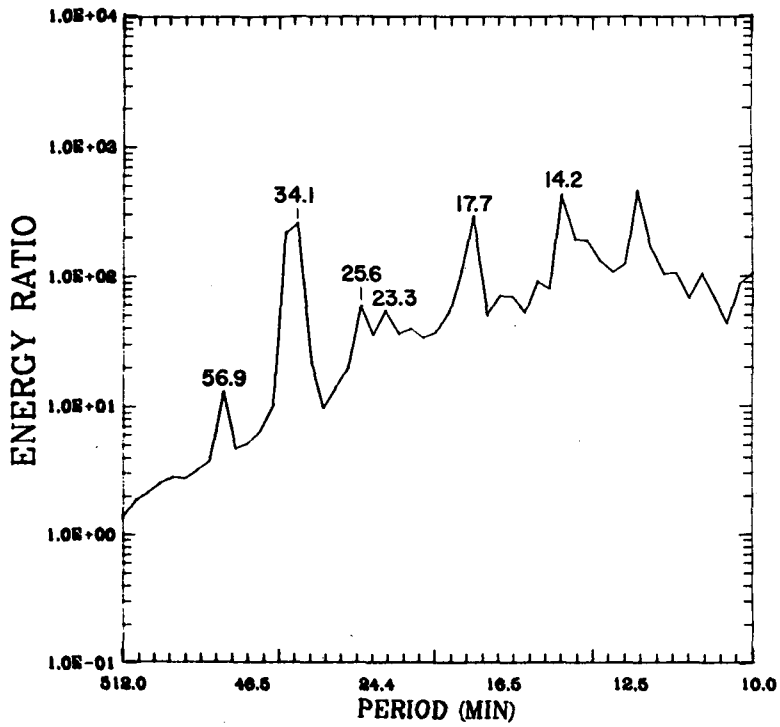

FIG. 1. Average response function for all 235 shoreline stations for pulse originating in Alaska region. Numbers above the peaks indicate wave period (min).

flat bottom outer "skirt" which both (4) and (5) require] and topography remained the same.

We obtained a measure of the overall response of the island system by calculating the arithmetic average of all 235 island shoreline response functions at each period. Fig. 1 (4) shows the result of this averaging process. Six response peaks stand out on this curve at periods above 12.5 min. In order of decreasing magnitude, these are located at 14.2, 17.7, 34.1, 25.6, 23.3 and 56.9 min. Peaks occurring below 12.5 min are ignored because waves below this period would have wavelengths shorter than three model grid intervals and thus could not be reliably resolved by the model. The period band centered on 36.6 min, which is adjacent to that centered on 34.1 min, consistently shows values nearly equal to the 34.1 min peak. This holds true on five of the six islands for which a peak occurs at one or the other period. Thus values at both of these periods will be listed.

Of the peaks listed above, only the 23.3 min peak did not appear in earlier work. However, peaks at 12.5, 16.0, 18.3, 20.5 and 73.1 min, all observed in the earlier model results, are not present now. The 73.1 min peak turned up in every previous island average response curve (Bernard, 1976), whereas no significant peaks at this period appear in the present results. This wave period falls within the range of the

TABLE 1. Values of averaged energy ratio for individual islands.

Island	Period (min) 56.9	36.6	34.1	25.6	23.3	17.7	14.2	Additional peaks (period/energy ratio)
Niihau	1	4	5	80	398	17	33	(19.7/23), (15.5/248), (13.1/70)
Kauai	2	4	4	20	68	2180	59	(13.8/161), (12.8/20)
Oahu	4	54	19	28	65	56	148	(22.3/106), (17.1/96), (13.5/117), (12.8/97)
Molokai	26	195	95	61	25	27	386	(21.3/54), (18.3/112), (16.5/159), (13.5/769)
Lanai	24	602	447	76	5	54	725	(16.5/117), (13.5/234)
Kahoolawe	44	514	878	138	4	37	916	(16.5/85), (15.1/139), (12.8/226)
Maui	32	602	984	130	28	67	575	(22.3/47), (16.5/116)
Hawaii	4	108	114	34	14	75	546	(21.3/23), (18.3/96), (16.0/68), (15.1/133), (13.1/194)
Weighted average	13	215	263	59	54	293	419	

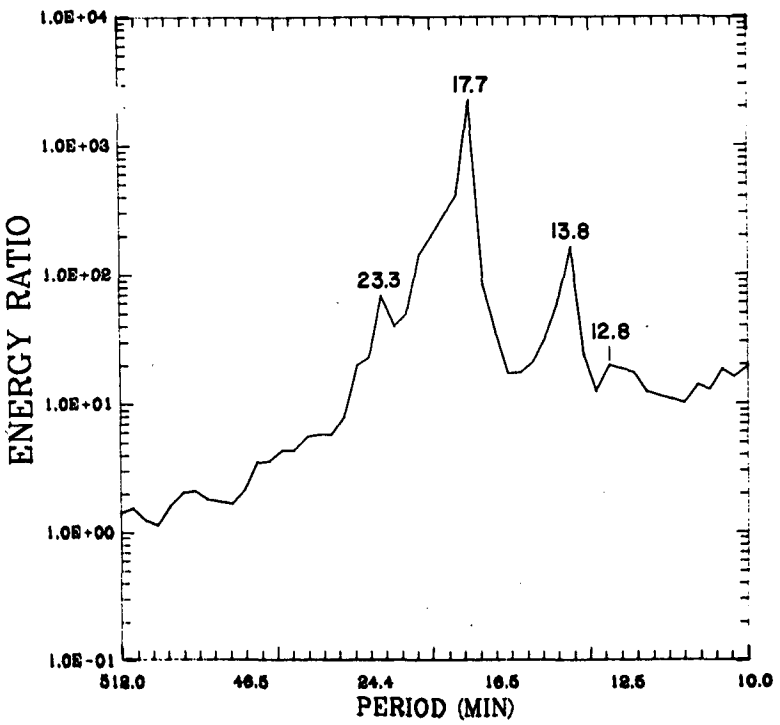

FIG. 2. As in Fig. 1 except around Kauai.

approximate travel times required for a wave front to reflect from the northern shores of the various islands, travel to the outer boundary, and return. This leads us to believe that the peak response may have been the result of reflections caused by the boundary condition (4). The loss of the other four peaks could indicate the reduction of reflections also, but the evidence is by no means as clear. The

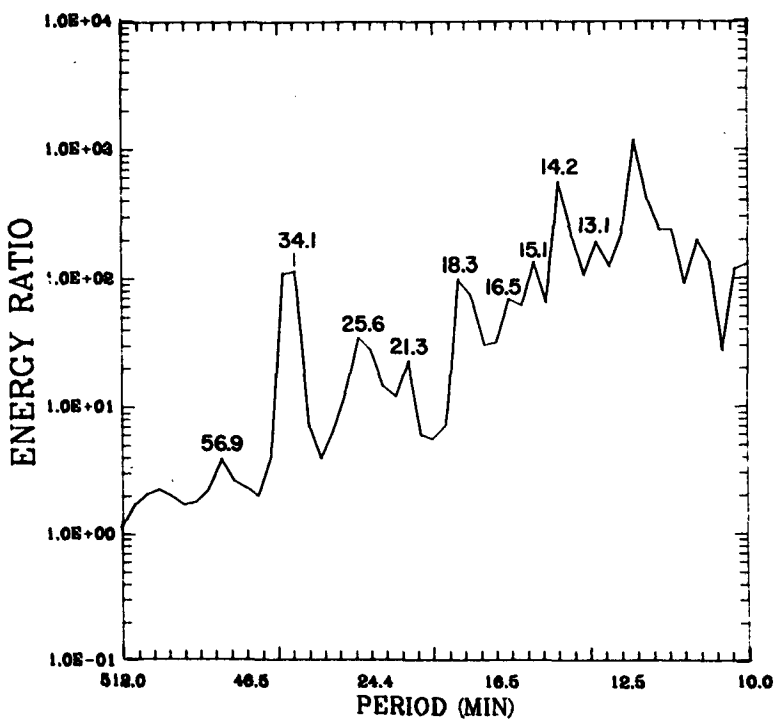

FIG. 3. As in Fig. 1 except around Hawaii.

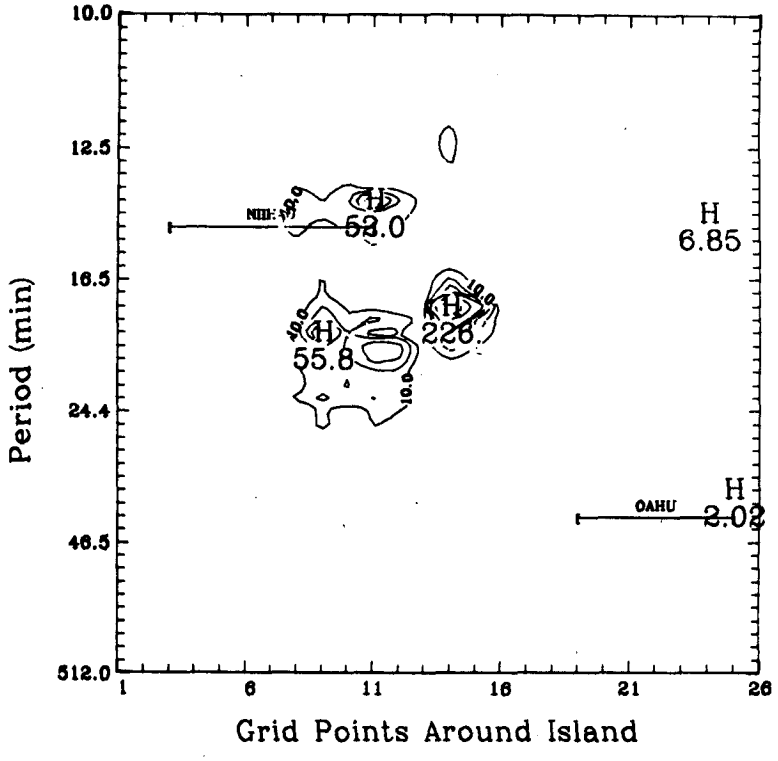

FIG. 4. Contours of (energy ratio)$^{1/2}$ around Kauai. The grid points are keyed to Fig. 6.

values listed in Table 1 represent both island and system average energy ratios at the peak periods observed in Fig. 1. Additional maxima on each island are also listed. Comparison between these values and those presented by Bernard and Vastano shows that, for the shared peak periods, only at 36.6 and

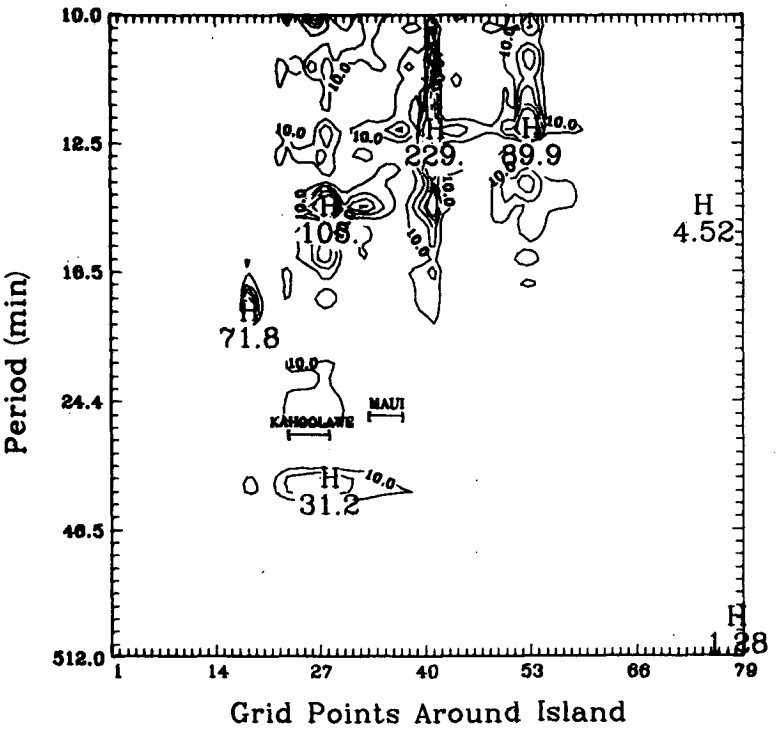

FIG. 5. As in Fig. 4 except around Hawaii.

17.7 min have the energy ratios increased in the new model version. Of course, the new peaks at 34.1 and 23.3 min also represent increases. All the other observed peaks showed a decrease in energy ratio. The implications are that the new boundary condition results in a general decrease in wave energy and a tendency toward stronger selective response at specific periods.

Kauai is the northernmost island in the chain. Its north coast is completely exposed to the incident waves and is partially sheltered from reflections from neighboring islands. The average response curve in Fig. 2 (5) shows the same features described above. The dominant response occurs at 17.7 min, as in the earlier study. But only two strong secondary resonances, 13.8 and 23.3 min, are evident. This stands in marked contrast to the eight secondary responses observed on Kauai by Bernard and Vastano. The 23.3 min peak occurs in both models, and the 13.8 min peak seen here is in a band adjacent to the 14.2 min band which contained an earlier peak. The Kauai curve is the most extreme example of strong energy response occurring in a small period band or bands, rather than spreading out through the spectrum.

Hawaii is the southernmost island in the chain. The response along its shore should be heavily influenced by reflections, since it is positioned southeast of the Molokai-Lanai-Kahoolawe-Maui group. Fig. 3 (5) shows the Hawaii response curve. Numerous response peaks are evident, and most of these are common to both old and new tests. The 14.2 min peak dominates in both cases, but the peak in the 36.6–34.1 min zone has shown a relative increase in the new results. The key fact in the new results is that two or three peaks are definitely stronger than the others, while in the earlier results the distinction between resonance strengths was less dramatic. Again, there seems to be less energy in the secondary peaks and more in the dominant peaks.

Bernard and Vastano analyzed contour plots of (energy ratio)$^{1/2}$ around the perimeter of each island and compared their results with actual data from the 1 April 1946 tsunami (Shepard *et al.*, 1950). Neither their test nor ours was executed specifically to simulate this tsunami (which had approximately the same approach azimuth as that used for the model), but several excellent correlations between the model results and the actual tsunami were observed. Figs. 4 (8) and 5 (9) show the contour plots drawn on the basis of the new results for Kauai and Hawaii. The horizontal bars in the plots serve a two-fold purpose: 1) the bar is located in the vertical at the period equal to the approximate travel time (over model topography) between the subject island and the island identified with the bar; and 2) the horizontal extent of the bar covers the portion of the island perimeter opposite the named island. The location of the island perimeter stations is portrayed in Fig. 6.

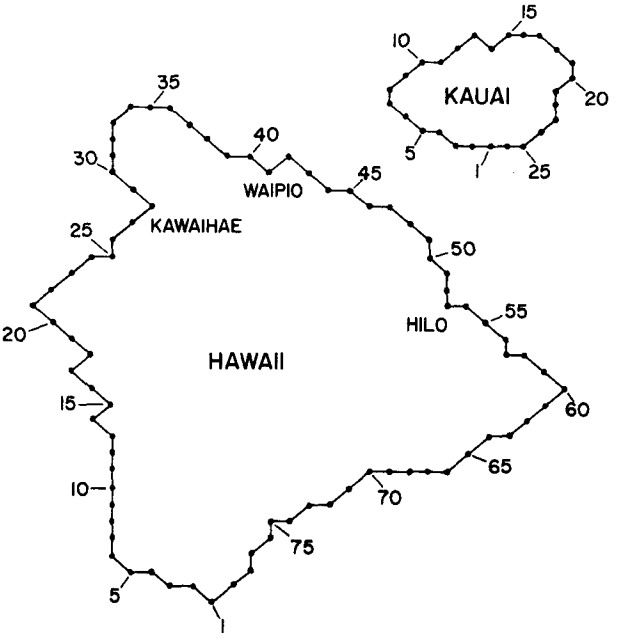

FIG. 6. Key for grid points around the model islands of Kauai and Hawaii.

The contours for Kauai are quite similar to the previous results. The strong response along the north coast, especially at Hanalei Bay (grid point 14) is evident. Discernible responses near the Kauai-Niihau travel time of 14.7 min occur along the west coast (grid points 3–11) and similar, though much less pronounced responses occur near the 40.0 min Kauai-Oahu travel time along the southeast coast. The major difference between the two runs is the absence, in the new test, of numerous small concentrations near to, but separate from, strong maxima. This serves to further underline the definition of a small number of major resonances seen in Fig. 2.

The Hawaii contours show the expected strong responses at Kawaihae Bay (grid point 28), Waipio Bay (grid point 41) and Hilo Bay (grid point 53). The response at Hilo is by far the strongest, as expected. Response at the Hawaii-Kahoolawe travel time is present. A local maximum response near the Hawaii-Maui travel time does occur, also, but at a level below the lowest contour level. As in the previous figure, the peak energy values have been sharply defined, with smaller peaks showing decreasing magnitudes. The stations on Hawaii tend to respond over a wider range of frequencies than do the stations on Kauai.

5. Conclusions

Earlier studies have shown that the finite-difference numerical model used in this study is a valuable tool for examining the tsunami response of a multiple-island system. The application of an improved outer boundary condition has not significantly altered the

major features of the original response results. However, the new boundary condition has accentuated primary resonances and suppressed secondary ones, which facilitates analysis of the model response. The model is now less susceptible to feedback due to reflections from the outer boundaries.

Acknowledgments. The authors would like to thank R. O. Reid and J. C. H. Mungall for sharing the results of their boundary condition research prior to publication. The funds for this study were provided in part by the Environmental Research Laboratories of the National Oceanic and Atmospheric Administration under NOAA Grant 04-7-022-44008 and in part by the National Weather Service. The computations were carried out at the National Center for Atmospheric Research, Boulder, Colorado. NCAR is sponsored by the National Science Foundation.

REFERENCES

Bernard, E. N., 1976: A numerical study of the tsunami response of the Hawaiian Islands. Ref. HIG-76-6, Hawaii Institute of Geophysics, University of Hawaii, 73 pp.

——, and A. C. Vastano, 1977: Numerical computation of tsunami response for island systems. *J. Phys. Oceanogr.*, **7**, 390–395.

Knowles, C. E., and R. O. Reid, 1970: The inverse tsunami problem for islands of simple shape. Ref. 70-7T, Dept. of Oceanography, Texas A&M University, 69 pp.

Longuet-Higgins, M. S., 1967: On the trapping of wave energy around islands. *J. Fluid Mech.*, **29**, 781–821.

Reid, R. O., and J. C. H. Mungall, 1980: A radiation condition for radially-spreading non-dispersive gravity waves. Submitted to *J. Phys. Oceanogr.*

Shepard, F. P., G. A. MacDonald and D. C. Cox, 1950: The tsunami of April 1, 1946. *Bull. Scripps Inst. Oceanogr.*, **5**, 391–528.

Vastano, A. C., and E. N. Bernard, 1973: Transient long wave response for a multiple island system. *J. Phys. Oceanogr.*, **3**, 406–418.

Observed and Predicted Great Lakes Winter Circulations

R. L. PICKETT

Great Lakes Environmental Research Laboratory, Ann Arbor MI 48104

18 September 1979 and 8 April 1980

ABSTRACT

Observed mean winter currents in Lakes Ontario and Huron are compared to predictions from a homogeneous, vertically integrated, steady-state model. If specific wind directions are selected to drive this model, the observed and predicted current patterns agree. The specific wind directions were chosen to maximize each lake's wind response. The agreement suggests that there is a mean wind-driven winter circulation in the Great Lakes, and that its pattern depends upon these specific wind directions. Based on these factors, winter circulations for Lakes Erie, Huron and Superior are predicted.

1. Introduction

Until 1972 there were no long-term observations of winter currents in the Great Lakes. There were, however, hypotheses about these currents. Surface cooling was expected to produce nearly isothermal water, so that with only weak density gradients, currents would be primarily wind-driven. Based on this hypothesis, numerous models were used to predict the wind-driven circulations of the Great Lakes. Both numerical (e.g., Gedney and Lick, 1970, 1972; Rao and Murty, 1970; Murty and Rao, 1970; Simons, 1971) and physical (e.g., Rumer and Robson, 1968) models were driven with a variety of winds. Even though these models predicted similar circulations when driven with similar winds, they could not be verified because of the lack of data.

By 1972 self-contained, automatic current meters with operational lives of over six months had been perfected. Instrumentation had improved to the point that circulation studies over a winter were possible. As a result, Canada and the United States cooperated on a Lake Ontario study using such instruments during winter 1972–73. Strings of meters were installed in November and retrieved in March. They operated continually, and the data from this study were reported by Pickett (1977).

Two years after this Lake Ontario study, the countries collaborated on another winter circulation study—this time on Lake Huron. Again automatic current meters were installed in autumn and retrieved in spring. Saylor and Miller (1979) reported the results of this 1974–75 winter study of Lake Huron.